OIKOS 85: 487–498. Copenhagen 1999

The spread of infection in seasonal insect-pathogen systems

Andrew White, Roger G. Bowers and Michael Begon

White, A., Bowers, R. G. and Begon, M. 1999. The spread of infection in seasonal insect-pathogen systems. – Oikos 85: 487–498.

Two distinct host-pathogen models with free-living infective stages and host movement are developed taking into account the fact that for many species the environment produces defined seasons. The models predict that a travelling wave of infection will sweep across the landscape, away from the point of pathogen introduction. Seasonality may reduce the range of disease spread compared to equivalent non-seasonal systems, and under certain circumstances the inclusion of seasonality is responsible for producing hollows in prevalence behind the wavefront. The models allow us to examine and challenge the conventional views of pathogen dispersal (in which so-called 'interference' of multiple waves from separate epicentres is sometimes invoked).

A. White, Inst. of Terrestrial Ecology, Edinburgh Research Station, Penicuik, Midlothian, UK EH26 0QB (awhite@ite.ac.uk). – R. G. Bowers, Dept of Mathematical Sciences, Univ. of Liverpool, P.O. Box 147, Liverpool, UK L69 3BX. – M. Begon, Population Biology Research Group, School of Biological Sciences, Univ. of Liverpool, P.O. Box 147, Liverpool, UK L69 3BX.

Empirical studies on the spatial spread of insect diseases are few, due mainly to the difficulties in observing clear patterns of dispersal in insect disease epizootics. The pattern of disease spread is most easily perceived in primary epizootics, but natural occurrences of these are rare and attempting to create a primary epizootic artificially is difficult since the spatial scale required is often very large. Studies which have been undertaken (Bird and Burk 1961, Stairs 1965, Young 1974, Otvos et al. 1987a, b) lack detailed descriptions of the patterns of dispersal, being concerned more with the mechanism of dispersal or the effectiveness of the pathogen as a biological control agent, or are undertaken for a short (one season) time period only (Dwyer and Elkinton 1995).

An exception to this is the study of Entwistle et al. (1983) on the spread of the nuclear polyhedrosis virus of *Gilpinia hercyniae* (GHNPV). Their observations and interpretations are widely accepted as portraying the expected pattern of disease dispersal in insects. They categorise disease dispersal into three phases. (1) A primary phase where disease prevalence decreases rapidly with distance from the epicentre. (2) A secondary phase characterised by a wave-like pattern in prevalence. This wave, however, may contain major and minor peaks, and in front of the wave, prevalence levels are low. (3) An interference phase where the wave form is lost and any pattern is less coherent. The prevalence in this third phase is now high over the entire landscape with, however, a suggestion of two or more peaks, possibly caused by interactions between multiple waves from several epicentres. A possible explanation for the occurrence of these peaks, framed not in terms of peaks themselves but the hollows between them, will be developed later in this article.

These results differ from those of Young (1974) on the spread of non-occluded baculovirus disease of *Oryctes rhinoceros* (ORBV) on the island of Tongutupa, Tonga Islands. Here a wave of disease travelled across the whole length of the island. *O. rhinoceros* has a continuous succession of overlapping generations which permits uninterrupted ORBV activity. A mathematical model by Dwyer (1994) for such a continuous system (one which excludes the effect of

Accepted 17 September 1998

ISSN 0030-1299

seasonality), which includes host movement to allow the disease to disperse, also predicts that (for certain parameter values) a wave of disease will travel across the entire landscape. The wave observed in the continuous systems studied by Young (1974) and Dwyer (1994) is different from that observed by Entwistle et al. (1983), since it contains no major and minor peaks (hence no hollows in prevalence). Also, neither of these studies suggests the possibility of an interference phase.

The system of Entwistle et al. (1983) differs from the systems in the Dwyer (1994) model and the Young (1974) study, in that *G. hercyniae* is highly seasonal. In particular, the host overwinters in a cocoon during which time there is no host-pathogen activity. Perhaps seasonality can account for the differences in the patterns of disease dispersal, and in particular, can account for the so-called interference phase and the formation of hollows in prevalence levels in the seasonal system. To test this, we outline two simple model strategies which describe opposite 'extremes' of seasonal behaviour. In the first, host birth can occur continuously throughout the duration of the season and in the second, all births occur instantaneously before the season. Neither of these two strategies provides an accurate description of real systems, but by examining these extreme scenarios the effect of seasonality alone, in comparison to results dependent on birth strategy, can be isolated. As Dwyer and Elkinton (1995) argue, such an approach can allow for exploration of otherwise untestable hypotheses.

The mathematical models

Since the host behaviour is dependent on a seasonal environment, the modelling will be approached in two stages. 1. Dynamics to represent the within-season activity of the host-pathogen system and host movement. 2. A representation of the overwinter behaviour where host-pathogen interactions do not occur and where hosts are no longer mobile.

Model 1: Continuous reproduction

In constructing the first model incorporating seasonality it was important to stay as close as possible – consistent with introducing the effect – to standard, non-seasonal models (Skellam 1951, Murray et al. 1986, Dwyer 1994), thereby allowing the effect of seasonality to be apparent. To this end, we consider the case where host reproduction can occur for the duration of the within-season period and where the dynamics, within this period, are represented by a reaction–diffusion model, combining an interspecific interaction (i.e. the 'reaction kinetics', to describe the interplay between host and pathogen) with diffusive movement (of the host).

Stage 1: Within season

The host-pathogen interactions will be described by Anderson and May's (1981) model G, but with the inclusion of a density-dependent term which models the effect of resource limitation on the host. We assume that this effect acts on the host birth rate in a manner linearly proportional to host density (see Bowers et al. 1993). Thus, the reaction model consists of three differential equations:

$$\frac{dX}{dt} = a(X+Y)(1-q(X+Y)) - bX - \nu WX, \quad (1)$$

$$\frac{dY}{dt} = \nu WX - (\alpha + b)Y, \quad (2)$$

$$\frac{dW}{dt} = \lambda Y - (\mu + \nu(X+Y))W. \quad (3)$$

Eqs (1)–(3) model the dynamics of a host within which the density of susceptible individuals is X and infected individuals is Y, and of a pathogen with a population of free-living infective stages of density W. The parameters a and b represent the intrinsic birth and death rate of the host respectively; α is the pathogenicity, that is the host death rate, in excess of b, attributable to the pathogen, while ν is the transmission efficiency of the pathogen between free-living infective stages and the host. The parameter λ is the rate at which free-living stages are produced by the host and μ is the decay rate of these stages. As is common practice, we set the recovery rate of the host to zero, since for insects, infection is generally fatal. Finally q is an intraspecific competition coefficient related to the carrying capacity, K, by $K = (a-b)/aq$.

The analysis of Bowers et al. (1993) shows that this system has three biologically relevant (i.e. non-negative population density) equilibrium points: the origin $(X, Y, W) = (0, 0, 0)$, the disease-free equilibrium $(K, 0, 0)$ and a coexistence equilibrium (X^*, Y^*, W^*). An analysis of the Jacobian of eqs (1)–(3) shows that the origin is always unstable, the disease-free equilibrium is stable if the inequality (4) (below) is reversed and the coexistence equilibrium is stable or replaced by stable limit cycles around the coexistence equilibrium (this depends on specific parameter choice) if

$$\lambda > (\alpha + \beta)\left(1 + \frac{\mu}{\nu K}\right). \quad (4)$$

This completes the description of the 'reaction kinetics' (see Appendix 1 for more detail).

If we add diffusion terms to the susceptible and infected classes to represent host movement, the reaction-diffusion equations are as follows:

$$\frac{\partial X}{\partial t} = a(X+Y)(1-q(X+Y)) - bX - vWX + D\frac{\partial^2 X}{\partial x^2}, \quad (5)$$

$$\frac{\partial Y}{\partial t} = vWX - (\alpha + b)Y + D\frac{\partial^2 Y}{\partial x^2}, \quad (6)$$

$$\frac{\partial W}{\partial t} = \lambda Y - (\mu + v(X+Y))W. \quad (7)$$

Here D is the diffusion coefficient which is a measure of the rate of host movement (assumed equal for healthy and infected hosts, as in Dwyer (1994)). Also, the previous system of ordinary differential equations has been transformed into a system of partial differential equations since the variables X, Y, W are now functions of both space, x and time, t. This approach is common for representing host movement (Skellam 1951, Murray et al. 1986, Dwyer 1994) and although it assumes space is one-dimensional it proves to be a reasonable approximation.

An important characteristic of reaction-diffusion models is their ability to exhibit 'travelling wave behaviour'. Analysis of the model (5)–(7), in conjunction with numerical studies, indicates that, for certain parameter values, travelling wave behaviour is possible. For our system this can be described as follows. Initially the population densities are at the disease-free equilibrium levels (i.e. $X=K$, $Y=0$, $W=0$) over the entire landscape. One point (say the origin) is invaded by a number of pathogen particles which start the epizootic. From this point a wave of infection will travel outwards, transforming populations from the disease-free equilibrium levels in front of the wave to those associated with the coexistence state in the wavetrain (see Dwyer (1994) for a similar result with a different model). From a combination of mathematical analysis and numerical studies (see Appendix 1), the wave solution can be shown to exist if

$$\lambda > (\alpha + b)\left(1 + \frac{\mu}{vK}\right). \quad (8)$$

Comparing (4) and (8) indicates that the wave solution exists if the coexistence equilibrium is stable (or replaced by stable cycles) for the temporal model (1)–(3). If this inequality is not satisfied (equivalent to instability of the coexistence equilibrium in the temporal model), then no wave is formed; the disease will disappear and the host will remain at the carrying capacity. Biologically this result implies that if the disease cannot invade at one point in space then it will not invade or spread over any points in space.

In host-pathogen systems which are not seasonal, the reaction-diffusion model (5)–(7) could be used to describe the entire dynamics. For a seasonal system, however, eqs (5)–(7) only describe the within-season dynamics (see below). The spatial scale is chosen large enough to allow the disease to spread for many generations before boundary conditions become important. It is assumed, initially, that there is a uniform population of susceptibles at the carrying capacity, at each point across the landscape (of length l m) and that this population is invaded by a large number of pathogen particles at the origin. We employ 'no flux' boundary conditions at the origin $\left(\frac{\partial X}{\partial x} = \frac{\partial Y}{\partial x} = \frac{\partial W}{\partial x} = 0\right)$ and require $(X, Y, W) = (K, 0, 0)$ where the domain ends at $x = l$ m. For our seasonal system, the dynamics described by (5)–(7) and the boundary condition will be relevant for each within-season period, but the initial conditions defined above are only relevant for the first season of modelling. The modelling begins in this first season, i.e. $t=0$, and is stopped at a time $t=t_1$, where t_1 represents the end of the first season. After this time, the modelling will move into the second, off-season, stage.

Stage 2: Overwinter

This second stage is required to represent the overwinter period, where no host-pathogen interactions take place and where there is no dispersal. This stage is represented as a discrete time step where the densities of healthy hosts and of the pathogen at the start of the next season are assumed to be a proportion of their respective densities at the end of the previous season. It is also assumed that no infected individuals will survive the overwinter period. These assumptions can be described mathematically as follows:

$$X(x, t'_{n+1}) = d_1 X(x, t_n), \quad 0 \le x \le l \text{ m}, \quad (9)$$

$$Y(x, t'_{n+1}) = 0, \quad 0 \le x \le l \text{ m}, \quad (10)$$

$$W(x, t'_{n+1}) = d_2 W(x, t_n), \quad 0 \le x \le l \text{ m}, \quad (11)$$

where t_n represents the time at the end of the nth season and t'_{n+1} the time at the start of the $(n+1)$th. The parameters d_1 and d_2 (assumed positive) represent the proportional overwinter survival of healthy host and pathogen, respectively. These equations will then generate the initial conditions for the dynamics representing the within-season activity (5)–(7) for each season after the first.

In the non-spatial set-up this representation of seasonality will have the effect of perturbing population levels at the beginning of each season. The stability of equilibria (or limit cycles) will not be affected, so populations will tend towards the stable state during the season and be perturbed away from this state by the overwinter dynamics.

Model 2: Instantaneous reproduction

Here, all reproduction will occur instantaneously before the season. To describe this some modifications are made to Model 1.

Stage 1: Within season

The model framework will remain as before except the host dynamics for the within-season period, eq. (5), become

$$\frac{\partial X}{\partial t} = -bX - \nu XW + D\frac{\partial^2 X}{\partial x^2}, \qquad (12)$$

where all terms are as defined earlier. This equation is used in conjunction with (6) and (7).

Stage 2: Overwinter

The equation representing the overwinter behaviour of healthy hosts, eq. (9), becomes

$$X(x, t'_{n+1}) = cd_1 X(x, t_n) f(d_1 X(x, t_n)), \quad 0 \le x \le l \text{ m}. \qquad (13)$$

Here, c represents the average number of viable eggs produced per adult, and $f(\cdot)$ is a density-dependent term representing interference (or competition) between adults (e.g. for egg laying sites), which is chosen such that $f(z) = \exp(-\kappa z)$.

Using this model formulation, the previous definition of the carrying capacity as the density of healthy hosts in the absence of disease is no longer applicable (since the density of hosts would not be constant). However, a pseudo carrying capacity can be defined whereby, in the absence of disease the densities at equivalent times in different seasons are the same. This pseudo carrying capacity can be set up so that it is stable under a disease-free perturbation in density. (The calculation of the pseudo carrying capacity and its stability properties is produced in Appendix 2.) With this formulation we only have one equilibrium (the origin) for the within season (stage 1) dynamics. Hence, the results concerning the existence of travelling waves no longer apply. However, when considered as a whole, Model 2 still has a pseudo coexistence point, or exhibits pseudo limit cycles for some parameter values (pseudo refers to the fact that an exact equilibrium is not reached). Thus, even though theoretical analysis cannot be undertaken, the possibility of a travelling wave connecting the two pseudo equilibria is still feasible.

Model setup

For both models, results are portrayed using parameter estimates for the *Gilpinia*–NPV system studied by Entwistle et al. (1983). These parameter values are used, at this stage, purely for illustrative purposes; however their use allows us to avoid repetition when the Entwistle et al. (1983) study is discussed later. The generality of the results to other parameter combinations is considered below. The parameter values employed are given in Figs. 1 and 4. (See Dwyer (1994) for the derivation of the stage 1 parameters, and Bird and Elgee (1957), Entwistle et al. (1983) and Olofsson (1987, 1988) for the original measurements). The stage 2 parameters need more consideration since seasonal models examining the spread of infection have not previously been proposed. The fate of the three classes,

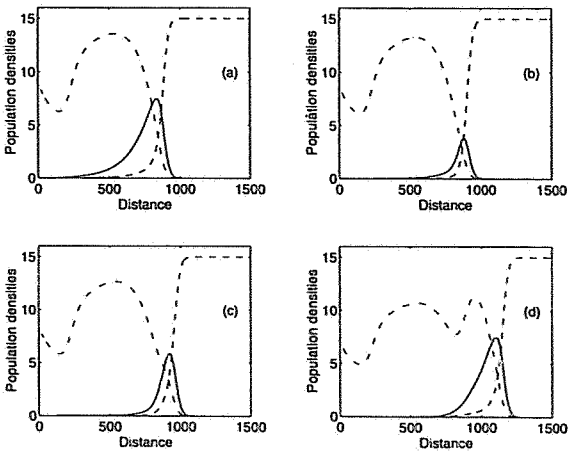

Fig. 1. The spread of infection in terms of susceptible hosts (m^{-2}) (– –), infected hosts (m^{-2}) (—) and pathogen particle $\times 0.6 \times 10^{-8}$ (m^{-2}) (– ·) for model 1. The portraits are depicted at a) the end of a season and b) 5 d, c) 10 d and d) 50 d into the next season. Parameters values are $a = 0.2917$ d^{-1}, $b = 0.2902$ d^{-1}, $\nu = 1.25 \times 10^{-8}$ m^2 d^{-1}, $\alpha = 0.05$ d^{-1}, $\lambda = 10^6$ d^{-1}, $\mu = 0.005$ d^{-1}, $K = 15$ m^{-2} and $D = 60$ m^2 d^{-1}.

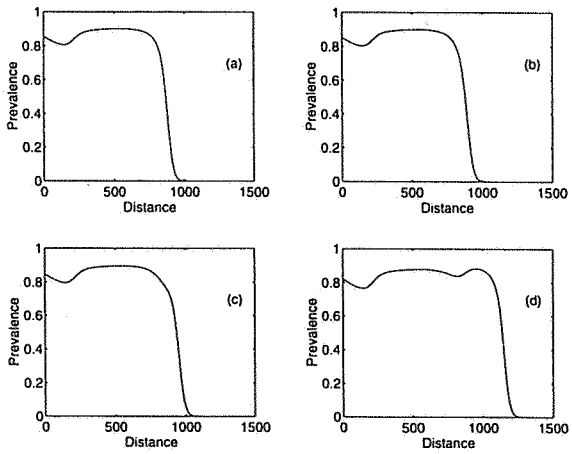

Fig. 2. The spread of infection represented in terms of the fraction of individuals infected for model 1. The portraits (a)–(d) are taken at times and with parameters corresponding those in Fig. 1.

X, Y, and W during the overwinter period will be considered in turn. The biological reasoning behind the model suggestions is taken from Zelezny (1976), Entwistle et al. (1983) and Briggs and Godfray (1996).

Susceptible individuals, X

Any susceptible individuals alive at the end of the season will be mature larvae and hence will form cocoons. This will happen at all points across the landscape. It is assumed that there is no loss of cocoons over winter and that adults emerge from all cocoons at the start of the next season. Hence, $d_1 = 1$. Tests, with $d_1 < 1$, representing cocoon loss over winter and/or only a proportion of cocoons emerging at the beginning of the season (diapause) can be shown to have a negligible effect on the model outcome.

Infected individuals, Y

Any infected individuals alive at the end of the season will die during the overwinter period. Hence, as defined in eq. (10), Y is set to zero for the start of the next season (see Briggs and Godfray (1996) for a similar approach but in a model without spatial structure). In addition it is assumed that infected larvae which did not release pathogen particles before the end of the season will die and not contribute any additional particles to the environment. One could approximate the effect of individuals containing some pathogen particles, but not infected sufficiently to lyse, by allowing the infecteds alive at the end of the season to produce pathogen particles at a reduced rate. We assume this reduced rate is zero.

Pathogen particles, W

The density of pathogen particle at the beginning of the season will be assumed to be equal to that remaining at the end of the previous season. Incorporation of overwinter decay of pathogen could be included, but this decay rate would be expected to be less than the within-season decay rate (Killick 1987) since pathogen particles are generally destroyed by UV radiation which is less severe overwinter (since UV intensity is dependent on solar inclination). Tests were undertaken where the proportional survival of the pathogen, d_2, was chosen to be 1, 0.75 and 0.5. For all cases the results were very similar (hence $d_2 = 1$ is chosen), and in particular the qualitative patterns and speed of spread were not altered. However, the number of seasons required for the population densities X, Y and W to approach their equilibrium values X^*, Y^* and W^* (see later) is reduced as d_2 is reduced.

The additional model 2, stage 2 parameter choices are defined to produce a stable pseudo carrying capacity and are detailed in Appendix 2.

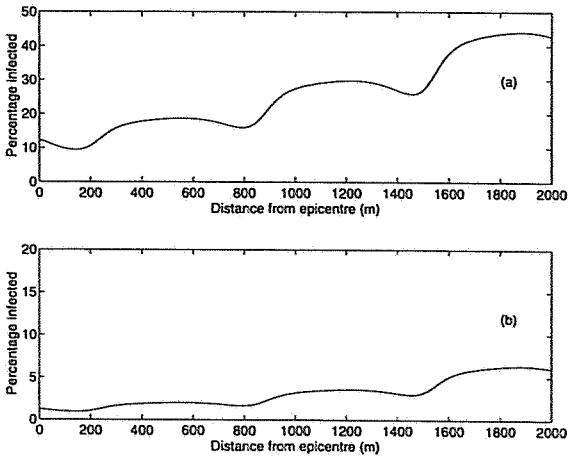

Fig. 3. The pattern of spread of the infection, in the wavetrain, in a) the 8th and b) the 12th generation (parameters as in Fig. 1).

Results: Model 1

Fig. 1 shows portraits of the output in terms of susceptible and infected hosts and scaled pathogen densities at the end of a season and at three times during the next season for model 1 (continuous reproduction). This portrait shows a wave of infection (clearly visible when viewed in terms of infected host density) moving away from the epicentre ($x = 0$). The difference in size of the maxima of infected individuals arises because the wave has to re-establish from zero infecteds over the land surface at the beginning of each season. It takes approximately 20 d before the wave of infection has been fully re-established. Fig. 1 also shows how the pathogen levels in the wavetrain slowly decay towards the coexistence equilibrium value W^*.

Fig. 2 displays how the progression of this wave will be observed if viewed in terms of prevalence. Hollows in prevalence are clearly visible and it transpires that a hollow will be formed in prevalence levels at the start of each season (after the first).

Comparing disease spread in seasonal and non-seasonal systems

1. Wave speed

An immediate question that arises when considering disease spread in seasonal and non-seasonal systems is whether the distance the disease will spread over a particular period of time will be affected by seasonality. In Appendix 1, we indicate how if a travelling wave is produced by the reaction-diffusion system (eqs 5-7) then there is a minimum speed, v_c, at which the wave must travel. This minimum speed is deduced using phase-plane analysis which indicates that wave solutions with speeds less than v_c are biologically unrealistic

since they produce negative population sizes. The actual speed at which the wave travels will be the same for seasonal and non-seasonal systems. In the hypothetical situation in which the wave of infecteds is fully re-established at the beginning of the season, the difference in distance of annual disease spread would only be dependent on season length (i.e. the seasonal model spread would be a fraction, (*seasonlength*)/365, of the non-seasonal model spread). However, an important aspect of the seasonal system is that there are no infected at the beginning of the season. As mentioned earlier, it takes approximately 20 d before the wave of infected is fully re-established. Skellam (1951) showed that the rate of advance of a wavefront is proportional to the number of individuals in the wavefront, so the wave speed may be reduced during the re-establishment period in our study, thereby reducing the range of disease spread further. Numerical results show that disease spread is limited by this process (Table 1), with the reduction in disease spread being more significant as the season length decreases.

II. Wave shape

The results for model 1, viewed in terms of prevalence of infection show defined hollows behind the wavefront (Fig. 2). These hollows are not observed in non-seasonal systems, since they are caused by the action of seasonality on the number of infected individuals. This becomes clear if we explain how a 'new' hollow is formed at the start of the season (the same process is responsible for the formation of those which are already evident). First, recall that the distribution of susceptibles and the pathogen at the end of the season, portrayed in Fig. 1a, becomes the distribution describing their initial conditions for the following season. The distribution of infecteds at the start of a season will be zero across the whole landscape. At the restart, the wave of infecteds is re-established (see Fig. 1b for 5 d into the season) but the 'size' of the wave is reduced compared with the wave at the end of the season. The wave continues to move away from the epicentre and gradually increases in size until the 'true' peak is re-established (Fig. 1c, d). The hollow in prevalence occurs in that part of the landscape over which the wave travels at the reduced level (approximately 700–900 m).

Table 1. A comparison of the range of pathogen spread for a continuous (non-seasonal) and seasonal version of Model 1. Parameters as in Fig. 1.

Time (d)	Distance of disease spread (m)		Difference (%)
	Continuous model	Seasonal model	
120	675	665	1.5
40	225	215	4.5
15	85	75	12

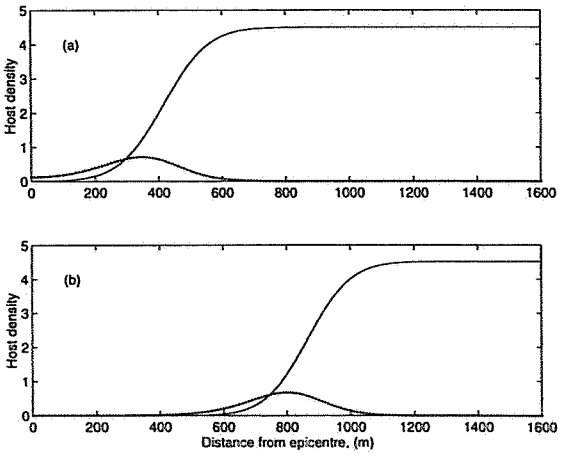

Fig. 4. The spread of infection in terms of susceptible (solid line) and infected (dotted line) densities against distance, depicted at the end of the season in which the pathogen is introduced and at the end of the following season for model 2 (instantaneous birth model). Parameter values are as in Fig. 1 except $c = 24$ eggs per adult, $b = 0.01$ d^{-1}, $\kappa = 0.439$, $\nu = 1.3 \times 10^{-9}$ m^2 d^{-1}, $D = 150$ m^2 d^{-1}.

The lower level of infecteds results in fewer pathogen particles being produced in this region, via the term λY (shown clearly in the hollow in pathogen levels in Fig. 1d). Hence, fewer susceptibles become infected via the transmission term νXW. Thus, the region contains higher than normal levels of susceptibles, generating the hollows in prevalence.

This process will occur at the wavefront at the start of every season. Thus, a new hollow will be formed at the wavefront for each overwinter period. The hollows will not propagate; they will remain over the same region of the landscape in which they were formed. The size of the hollows portrayed in Fig. 1 are determined by the speed at which the infection levels can become re-established. If the transmission coefficient ν is higher, the wave re-establishes faster and hence the hollows are less obvious. Note too that the hollows are not caused by cyclic or oscillatory dynamics in population densities in the wavetrain. Hollows from such a process are possible (if the non-spatial dynamics are cyclic or oscillatory), but in contrast to the model results they would not stay fixed in one position on the landscape and their frequency would not be expected to be one per season.

III. Long-term predictions

Fig. 3 shows portraits of the prevalence levels of infecteds in the wavetrain at the end of the 8th and 12th generations. As the population densities of the susceptible and infected hosts tend towards their coexistence steady state of X^* and Y^* (for some parameter values this steady state is replaced by values associated with stable cycles), so the prevalence levels will tend towards a constant value $P^* = Y^*/(X^* + Y^*)$. This trait is also

observed in non-seasonal spatial versions of the model, but the populations would reach the equilibrium values in a shorter time. For our parameter values $P^* \approx 0.02$ and Fig. 3b shows how this value is approached by about the 12th generation. However, this does not imply that there are large numbers of susceptible individuals and small numbers of infecteds since total population densities in the wavetrain are very low, approximately 2.5% of the host densities before the introduction of disease. This result is in good agreement with the study of Bird and Elgee (1957) who estimated mortality levels of approximately 98–99%, in larval populations of *Gilpinia* in Canada, after the introduction of NPV.

Generality of results

The result that a single wave of infection will spread from the initial focus will generalise to all parameter combinations that satisfy the inequality (4). If this inequality is not satisfied, the disease will die out and no wave pattern will emerge. In situations where a wave does emerge, the observation of hollows, produced at the beginning of each season, will be robust. However, the precise size of the hollows may vary according to parameter choice. The result that in the long term, the observed levels of individuals behind the wavefront will settle to that associated with the coexistence levels or levels associated with stable limit cycles around the coexistence equilibrium is also robust.

Results: Model 2

Fig. 4 shows the results in terms of host densities at the end of successive seasons for the model with instantaneous birth (Model 2). A single wave of infection, travelling away from the point of pathogen introduction is responsible for disease spread. This wave will be apparent provided the disease can become established (although it is not possible to detail an expression which describes when this occurs). If a wave is observed then the density in the wavetrain will tend towards a pseudo coexistence equilibrium or values associated with a pseudo limit cycle. If the disease cannot establish the host will remain at the pseudo carrying capacity at all points on the land surface. Thus, a direct link between these results and those for the model with continuous reproduction can be drawn, even though the model set-ups describe opposite extremes of seasonal behaviour. In addition to the difference in reproductive strategies the position of density-dependence is also different between the two models (being coupled to the infection dynamics in model 1 and before the infection dynamics in model 2). These variations cause differences in the behaviour in the wavetrain (since the behaviour in the wavetrain is determined by the reaction dynamics. Hence, differences between model 1 and 2 may result from population values tending towards exact or psuedo equilibrium values respectively). However, the similarity between travelling wave behaviour is striking. Thus, it is reasonable to hypothesise that the same underlying mechanism is responsible for producing the travelling wave behaviour in both models.

The production of hollows in prevalence levels is not observed for model 2 (Fig. 5). The hollows in prevalence disappear as a direct result of introducing birth as a discrete process. Under this assumption, it is simple to see that the distribution profile of susceptibles at the beginning of the season is of higher density, at each point on the landscape than the corresponding profile at the end of the previous season. This higher susceptible density allows the wave to regenerate 'unconstrained' from the position in which it was halted in the previous generation. In the original seasonal setup, the regeneration of the infected wave was constrained by the profile of the susceptible distribution at the end of the previous generation, causing a gap in the landscape over which the wave travelled, which in turn caused hollows in prevalence.

If we consider non-seasonal infection in model 2 by allowing instantaneous births without the infected class being set to zero, then seasonality will reduce the range of disease spread for model 2 in a similar manner to that described for model 1.

Discussion

The two models, describing contrasting ways of representing host reproduction in a seasonal environment, predict that the pathogen will spread as a result of a

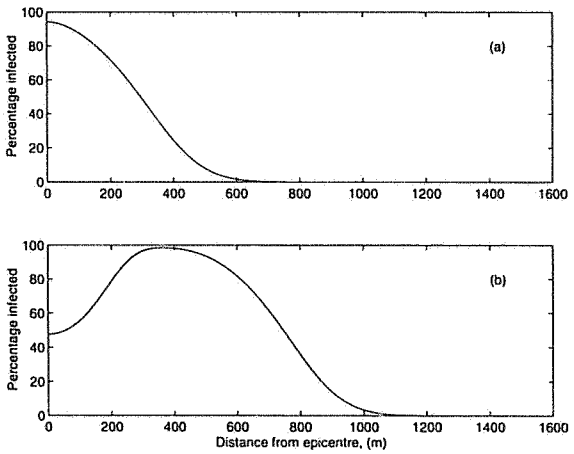

Fig. 5. The spread of infection represented in terms of the fraction of individuals infected for model 2. The portraits are taken at times and with parameters corresponding those in Fig. 4.

single travelling wave of infection from the initial epicentre. This result parallels the findings of non-seasonal approaches (Dwyer 1994), suggesting that seasonality will not affect the process of disease spread. However, seasonality will affect the range of disease spread (Table 1), with this effect becoming more significant as the season length decreases. In some circumstances seasonality may affect the shape of the wavetrain (Fig. 2).

Can the travelling wave description predicted by the models explain the patterns of disease spread observed in real systems? There are several empirical studies concerned with the spread of infection in seasonal systems (Bird and Elgee 1957, Bird and Burk 1961, Stairs 1965, Otvos et al. 1987a, b), and it is often suggested that the pathogen spreads as a propagating wave. However, detailed descriptions of the spread are not reported in the above studies, and the only comprehensive study, where patterns of spread are clearly outlined was undertaken by Entwistle et al. (1983). Their observations and interpretations are widely accepted as portraying the expected pattern of disease dispersal in insects. As detailed earlier, the model parameters used above are approximations of the *Gilpinia*–NPV system studied by Entwistle et al. (1983), although this system lies somewhere between the two model representations, as births occur for a period at the start of the season.

Entwistle et al.'s (1983) results for the spread of NPV virus of *Gilpinia* (Fig. 6) show the progression of a wave from an epicentre, although by the third season (Fig. 6b) Entwistle et al. (1983) claim that the wave pattern has disappeared, since the prevalence is now high over the entire transect. They termed this the interference phase. They argue that their observed behaviour can be explained by the fact that, as such a disease focus grows it will generate discontinuous satellite outbreaks beyond its confines, with the interference pattern generated by many such disease centres overlapping and interacting. In contrast, both models here predict that disease spread will result from the movement of a single wave of infection. Model 1 predicts the occurrence of hollows in the prevalence levels which may give the impression of multiple wave interference, but which are actually caused by the action of seasonality on the propagating wave of infection, but model 2 does not predict hollows. Could seasonality explain the so-called interference phase without the need to implicate separate epicentres of infection?

Perhaps a more sophisticated modelling strategy is required to fully address this conflict between the model results, whereby processes such as age structure, and/or a separate adult class could be included and where birth could occur for a period at the beginning of the season. Nevertheless, the model results do challenge the existence of an interference phase, suggesting that a single wave of infection is the most likely cause of disease dispersal in host-pathogen systems such as Entwistle et al.'s (1983), regardless of whether hollows are caused by seasonality, by an alternative biological mechanism or whether they are just a sampling artefact in the empirical study. Evidence of this can be obtained from Entwistle et al.'s (1983) results. They remark that by the end of the second season (October 1972) the density of individuals in the nearest 600 m to the epicentre is so low that accurate estimation of prevalence cannot be made. If disease spread were the result of a single wave then the population density would be expected to be low in this region (Figs. 1 and 3). Also, Entwistle et al. (1983) question why they cannot observe the wave further from the epicentre in the third season, and due to its absence they introduce the interference phase in which disease spread occurs via the translation of discrete foci of infection with limited diffusion-like dispersal around each focus. Even if this is the case, it is hard to see why such a process would not always have a leading, wave-like edge at the position where infection is furthest from the original focus (at least until boundary conditions become significant). Such a leading edge would be observed beyond the study range in Entwistle et al.'s (1983) portrait for the third season (Fig. 6a). Thus, although our models do not attempt to be definitive descriptions of their study system, our results do suggest alternative, plausible explanations for Entwistle et al's (1983) observations.

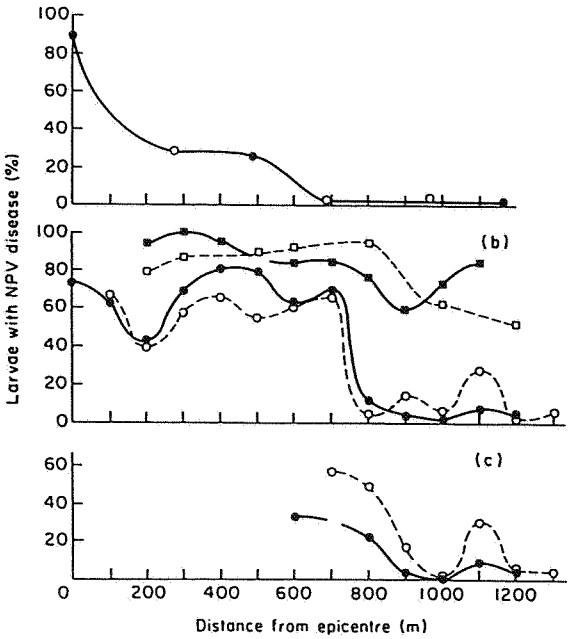

Fig. 6. Patterns of spread of *Gilpinia hercyniae* NPV disease at Afon Biga 1971–73 taken from Entwistle et al. (1983). (a) October 1971 (●, NE transect; ○, SW transect). (b) September 1972 (●, NE transect; ○, SW transect) and September 1973 (■, NE transect; □, SW transect). (c) October 1972 (●, NE transect; ○, SW transect). Where data points have not been joined larval samples were too low for an accurate estimation of disease prevalence.

Such an approach has been exploited by Dwyer and Elkinton (1995) who conduct a large-scale study on the spread of NPV in gypsy moth (*Lymantria dispar* (L.)) populations. Their study is for one within-season period only, and hence comparisons with the models presented here is limited. However, they report that movement of infected larvae is important in spreading the disease, and that prevalence of disease decreases with distance from the epicentre. This is very similar to the pattern that would be observed for both models 1 and 2 if only one within-season period is considered (see Fig. 5a), suggesting that a wave of infection may be an important disease dispersal mechanism.

The current study has shown how 'strategic' spatial models can be adapted in a novel fashion in order to extend the debate on the mechanisms and methods by which disease may spread in natural systems. It also highlights how specialised analysis of temporal and spatial models of host-pathogen systems could be used in parallel with experimental and field studies to help explain the details of disease spread in real systems.

References

Anderson, R. M. and May, R. M. 1981. The population dynamics of microparasites and their invertebrate hosts. – Philos. Trans. R. Soc. Lond. B 291: 451–524.

Bird, F. T. and Burk, J. M. 1961. Artificially disseminated virus as a factor controlling the European Spruce sawfly, *Diprion hercyniae* (Htg.) in the absence of introduced parasites. – Can. Entomol. 93: 228–238.

Bird, F. T. and Elgee, D. E. 1957. A virus disease and introduced parasites as a factor of controlling the European Spruce sawfly, *Diprion hercyniae* (Htg.) in central New Brunswick. – Can. Entomol. 89: 371–378.

Bowers, R. G., Begon, M. and Hodgkinson, D. E. 1993. Host-pathogen population cycles in forest insects? Lessons from simple models reconsidered. – Oikos 67: 529–538.

Briggs, C. J. and Godfray, H. C. J. 1996. The dynamics of insect-pathogen interactions in seasonal environments. – Theor. Popul. Biol 50: 149–177.

Dwyer, G. 1994. Density dependence and spatial structure in the dynamics of insect pathogens. – Am. Nat. 143: 533–562.

Dwyer, G. and Elkinton, J. S. 1995. Host dispersal and the spatial spread of insect pathogens. – Ecology 76: 1262–1275.

Entwistle, P. F., Adams, P. H. W., Evans, H. F. and Rivers, C. F. 1983. Epizootiology of a nuclear polyhedrosis virus (baculoviridae) in European Spruce sawfly (*Gilpinia hercyniae*): spread of disease from small epicentres in comparison with spread of baculovirus diseases in other hosts. – J. Appl. Ecol. 20: 473–487.

Killick, H. J. 1987. Ultra-violet light and *Panolis* nuclear polyhedrosis virus: a non-problem? – In: Leather, S. R., Stoakley, J. T. and Evans, H. F. (eds), Population biology and control of the pine beauty moth. HMSO, London, pp. 69–76.

May, R. M. 1974. Stability and complexity in model ecosystems. – Princeton Univ. Press, Princeton, NJ.

Murray, J. D., Stanley, E. A. and Brown, D. L. 1986. On the spatial spread of rabies among foxes. – Proc. R. Soc. Lond. B 229: 111–150.

Olofsson, E. 1987. Mortality factors in a population of *Neodiprion sertifer* (Hymenoptera: Diprionidae). – Oikos 48: 297–303.

Olofsson, E. 1988. Environmental persistence of the nuclear polyhedrosis virus of the European pine sawfly in relation to epizootics in Swedish Scots pine forests. – J. Invertebr. Pathol. 52: 119–129.

Otvos, I. S., Cunningham, J. C. and Friskie, L. M. 1987a. Aerial applications of nuclear polyhedrosis virus against Douglas-fir tussock moth, *Orgyia psuedotsugata* (McDunnough) (Lepidoptera: Lymantriidae). I. Impact in the year of application. – Can. Entomol. 119: 697–706.

Otvos, I. S., Cunningham, J. C. and Alfaro, R. I. 1987b. Aerial applications of nuclear polyhedrosis virus against Douglas-fir tussock moth, *Orgyia psuedotsugata* (McDunnough) (Lepidoptera: Lymantriidae). II. Impact 1 and 2 years after application. – Can. Entomol. 119: 707–715.

Skellam, J. G. 1951. Random dispersal in theoretical populations. – Biometrika 38: 196–218.

Stairs, G. R. 1965. Artificial initiation of virus epizootics in Forest tent caterpillar populations. – Can. Entomol. 97: 1059–1062.

Young, E. C. 1974. The epizootiology of two pathogens of the coconut palm rhinoceros beetle. – J. Invertebr. Pathol. 24: 82–92.

Zelezny, B. 1976. Transmission of a baculovirus in populations of *Oryctes rhinoceros*. – J. Invertebr. Pathol. 27: 221–222.

Appendix 1

To re-iterate the results in the main text, the reaction kinetics, eqs (1)–(3), have three equilibria, the origin, the disease-free equilibrium (K, 0, 0) and the coexistence equilibrium (H^*, Y^*, W^*), where the total host density $H^* = X^* + Y^*$. The analysis below will be conducted using (H, Y, W) but conversion to X can be made at any time via the translation $X = H - Y$. The coexistence equilibrium is defined explicitly as

$$H^* = \frac{(\Gamma\alpha - \lambda(\alpha - r))K}{2\lambda r} + \frac{1}{2}\left\{\left(\frac{(\Gamma\alpha - \lambda(\alpha - r)K)}{\lambda r}\right)^2 + \frac{4\Gamma\mu\alpha K}{\lambda\nu r}\right\}^{\frac{1}{2}},$$

$$Y^* = \frac{r}{\alpha} H^*\left(1 - \frac{H^*}{K}\right),$$

$$W^* = \frac{\lambda Y^*}{\mu + \nu H^*}. \qquad (14)$$

Here, $\Gamma = a + b$. This coexistence equilibrium is biologically relevant (in the sense that $H^* \geq Y^* > 0$ and $W^* > 0$) if

$$\lambda > (\alpha + b)\left(1 + \frac{\mu}{\nu K}\right). \qquad (15)$$

From an analysis of the Jacobian (or standard linearisation May (1974)) of eqs (1)–(3) it can be deduced that the coexistence equilibrium is stable or replaced by stable limit cycles around the coexistence equilibrium if the inequality (15) is satisfied. Thus, whenever the coexistence equilibrium is biologically relevant it is also

stable or replaced by stable oscillations. Furthermore, if this inequality is reversed, it can be shown that the coexistence equilibrium is unstable when it is not biologically relevant, and also that this is when the disease-free equilibrium is stable. (See Bowers et al. (1993) for a more detailed explanation.)

Calculating a threshold for disease spread in Model 1

Numerical solutions to eqs (5)–(7) support the biological expectation of a wave transforming the population densities from the spatially uniform disease-free equilibrium into the coexistence equilibrium of the reaction only model, eqs (1)–(3). Waves of this kind travel with constant shape and speed, so when viewed on a travelling co-ordinate system moving in the same direction and at the same speed, it will appear stationary. This can be achieved mathematically by making the change of variable substitution $\xi = x + vt$, where v is the rate of advance of the wave of disease. This converts the partial differential equations that are functions of space, x, and time, t, to ordinary differential equations that are a function of the new variable, ξ. Incorporating this transformation, the eqs (5)–(7) become

$$vH' = rH\left(1 - \frac{H}{K}\right) - \alpha Y + DH'', \tag{16}$$

$$vY' = \nu W(H - Y) - \Gamma Y + DY'', \tag{17}$$

$$vW' = \lambda Y - (\mu + \nu H)W, \tag{18}$$

where $'$ represents differentiation with respect to ξ. This second order system can be simplified further to a first order system by the introduction of two new variables I and J such that $H' = I$ and $Y' = J$ and substitution results in the following system:

$$H' = I, \tag{19}$$

$$I' = \frac{1}{D}\left(vI - rH\left(1 - \frac{H}{K}\right) + \alpha Y\right), \tag{20}$$

$$Y' = J, \tag{21}$$

$$J' = \frac{1}{D}(vJ - \nu W(H - Y) + \Gamma Y), \tag{22}$$

$$W' = \frac{\lambda}{v} Y - \frac{\mu + \nu H}{v} W. \tag{23}$$

This system of equations has three biologically relevant equilibrium states with respect to ξ, corresponding to uniformity in space and constancy in time. These equilibrium states are: $(H, I, Y, J, W) = (0, 0, 0, 0, 0)$, $(K, 0, 0, 0)$ and $(H^*, 0, Y^*, 0, W^*)$, where K is the carrying capacity and H^*, Y^*, W^* are as defined in eq. (14). From the analysis of the reaction kinetics we know that the final equilibrium in this list is biologically relevant if and only if inequality (15) is satisfied. A travelling wave solution is a trajectory from $(K, 0, 0, 0, 0)$ to $(H^*, 0, Y^*, 0, W^*)$, providing H, Y, W are positive. Thus, eq. (15) must again be satisfied.

Information about the existence of this travelling wave can be obtained from an analysis of the eigenvalues of eqs (19)–(23) linearized around the equilibrium $(K, 0, 0, 0, 0)$. The eigenvalues, z, can be obtained by solving the characteristic polynomial

$$(z^2 - zvD^{-1} - D^{-1}r)h(z) = 0. \tag{24}$$

Here

$$h(z) = z^3 + Az^2 + Bz + C, \tag{25}$$

and

$$A = \frac{\mu + \nu K}{v} - \frac{v}{D}, \tag{26}$$

$$B = \frac{-(\Gamma + \mu + \nu K)}{D}, \tag{27}$$

$$C = \frac{1}{vD}(\lambda \nu K - \Gamma(\mu + \nu K)). \tag{28}$$

The quadratic factor of the characteristic polynomial produces the two eigenvalues associated with a trajectory in a subspace where there are no infecteds or pathogen present. These eigenvalues combine with 'corresponding' eigenvalues at the origin to produce the possibility of a travelling wave from the origin to the infection-free equilibrium in a subspace devoid of infecteds and pathogen. Since the initial conditions for the host is a spatially uniform population of susceptibles which is already at the carrying capacity, such a travelling wave could not be realised here.

Since the quadratic factor of (24) can be discounted it is possible to deduce that if we are to have a travelling wave, caused by a heteroclinic orbit leaving the disease-free equilibrium, then this orbit must leave via the unstable subspace created by the eigenvectors associated with the positive roots of $h(z)$. It is therefore useful to examine $h(z)$ for the possibility of positive roots. From eq. (27) we can deduce that $B < 0$ and eq. (28)

$$\Rightarrow C > 0 \quad \text{if} \quad \lambda > (\alpha + b)\left(1 + \frac{\mu}{\nu K}\right).$$

This is the same requirement as eq. (15) implying that $C > 0$ whenever the coexistence equilibrium is biologically relevant. Using this and the definition of $h(z)$ (eq. 25), we can determine the following properties:

$h(\pm\infty) = \pm\infty$,

$h'(0) = B < 0$,

$h(0) = C > 0$ if $H^*, Y^*, W^* > 0$.

A sketch of $h(z)$, taking into account the above properties would reveal that there is always one negative real root, and that we move from having a complex conjugate pair of real roots, to a repeated positive real root, to different positive real roots, as C is decreased from $\infty \to 0$. When complex roots occur it implies that the solution near the critical point will oscillate. Since, in this instance, $Y, W = 0$ at critical point, oscillations will produce negative population sizes. Thus, although a wave solution exists it will produce unrealistic negative population sizes. So, we require all roots to be real, implying that C must not exceed a maximum value. For fixed parameters this is equivalent to requiring that v, the wave speed, exceeds a minimum value v_c (since increasing v from 0 means C decreases from ∞ (eq. (28)). The minimum wave speed v_c occurs when $h(z)$ has coincident roots, or equivalently when there is a z such that $h'(z) = 0$ and $h(z) = 0$. Using these results z can be eliminated from eq. (25) to find v_c in terms of the other parameters. In terms of proving the existence of a travelling wave, this is as much detail as can be determined from theoretical investigation (see Dwyer 1994 for a similar approach). However, the information deduced here can be used to direct numerical investigations.

Numerical experiments reveal that whenever $C > 0$ a travelling wave is observed converting population densities from the disease-free equilibrium values to those of the coexistence or limit cycles around the coexistence point. If $C < 0$, i.e. when the coexistence is not biologically relevant, then no wave occurs and the population remains at the disease-free equilibrium level over the entire landscape. Thus, it seems reasonable to hypothesise that the travelling wave emanates from the unstable subspace created by the eigenvectors associated with the positive roots of $h(z)$ when $C > 0$. Moreover, the criteria for determining the sign of C are the same as that determining the biological relevance and stability of the coexistence equilibrium in the non-spatial model (eqs 1–3). Thus, connections can be drawn between travelling wave existence in the reaction-diffusion model (eqs 5–7) and stability of equilibria in the non-spatial model. If the 'reaction kinetics' imply that the disease-free state is stable and the coexistence point unstable, then there is no travelling wave between the equilibria in the reaction-diffusion model and population levels stay at the disease-free state. If however the reaction kinetics suggest that the disease-free state is unstable, and the coexistence point is either stable or stable cycles are expected then a travelling wave will be present. Biologically, this implies that if the pathogen cannot survive in one point in space, then it will not survive or spread in space.

Appendix 2

Outlined below is the method by which the stable pseudo carrying capacity is calculated for model 2 where reproduction is instantaneous. In the absence of infection, the dynamics for the whole season in model 2 are as follows:

Let X_n^0 represent the density of healthy hosts at the beginning of generation n and let X_n^s be the density at the end of the within-season period of length s. Then from eqs (12), but disregarding infection and diffusion

$$X_n^s = \exp(-bs)X_n^0,$$

$$= \sigma X_n^0, \tag{29}$$

and from (13)

$$X_{n+1}^0 = cd_1 X_n^s \exp(-\kappa d_1 X_n^s). \tag{30}$$

Combining (29) and (30) gives

$$X_{n+1}^0 = cd_1\sigma X_n^0 \exp(-\kappa d_1 \sigma X_n^0). \tag{31}$$

Here, eq. (31) represents the infection-free dynamics from the beginning of one season to the beginning of the next. This equation has one non zero equilibrium, X^*, where

$$X^* = \frac{\ln(cd_1\sigma)}{\kappa d_1 \sigma} \tag{32}$$

This equilibrium is stable when the absolute value of the derivative of the right hand side of eq. (31), evaluated at X^*, is less than 1. Mathematically, the equilibrium is stable if

$$|cd_1\sigma \exp(-\kappa d_1 \sigma X^*)[1 - \kappa d_1 \sigma X^*]| < 1, \tag{33}$$

from (32)

$$\Leftrightarrow |(1 - \kappa d_1 \sigma X^*)| < 1, \tag{34}$$

$$\Leftrightarrow |1 - \ln(cd_1\sigma)| < 1. \tag{35}$$

From eq. (35), the condition for stability can be expressed simply as

$$cd_1\sigma < \ln 2. \tag{36}$$

Since $d_1 = 1$ and $\sigma = \exp(-1.2) = 0.301$ (since $b = 0.01$ chosen somewhat arbitrarily to allow 30% of larvae to

survive in the absence of infection and the season length $s = 120$, we choose $c = 24$ so that the equilibrium is stable and c is as close to values predicted for the empirical system as possible (*Gilpinia* are expected to produce 30–40 viable eggs per adult). With these parameters set, $\kappa = 0.4387$ is chosen, so that the actual value of the equilibrium $X^* = 15$ (since this was the value at the carrying capacity in the original seasonal model).